Influence of Viscoelastic Dampers on the Ground Resonance Instability of Helicopters

Leonardo Sanches
Domingos Alves Rade
UFU - Universidade Federal de Uberlândia, Faculdade de Engenharia Mecânica, Laboratório Mecânica de Estruturas Prof. José Eduardo Tannús Reis
ls.leonardosanches@gmail.com, domingos@ufu.br

Abstract. *The ground resonance phenomenon has been studied in the last decades in order to advance the comprehension and to find out means to prevent helicopters from unstable oscillations. Elastomeric dampers have been the preferred devices employed to reduce such instabilities rather than conventional hydraulic dampers. Recent studies have devoted their attention to the investigation of the influence of the aging effects on the boundaries of the instability. The introduction of blade-to-blade dissimilarities creates new unstable zones. The present work aims at analyzing the instability of helicopters having the elastomeric dampers in the fuselage and blades. A parametric study is developed for analyzing the influence of different dissipative power of dampers on the boundaries of the instability. The treatment of the governing equations with time dependent coefficients are conducted by using the Method of Multiple Scales.*

Keywords: Viscoelastic Material, Parametric Instability, Method of Multiple Scales, Fractional Derivative Viscoelastic Model

1. INTRODUCTION

Attention has been devoted in the literature on the study of the stability of helicopters when they are on the ground. The ground resonance instability can be accurately predicted for hinged and bearingless rotor by using the linearized periodic equations of motion (Donham *et al.*, 1969; Lytwyn *et al.*, 1971; Hodges, 1979).

Recent studies verify the influence of blade-to-blade dissimilarities on the boundaries of the ground resonance (Wang and Chopra, 1992; Gandhi and Malovrh, 1999; Sanches *et al.*, 2011, 2012). The rotor asymmetries might be caused by the aging effects and it is modeled by altering the lag stiffness. Depending on the level of blade dissimilarities, new instability regions are found.

The appearance of these new instability regions is studied in (Sanches *et al.*, 2012).The periodic governing equations of the ground resonance phenomenon is interpreted as a parametrically excited system. Studies showed the existence of parametric resonances, in which some are unstable (Dufour and Berlioz, 1998; Driot *et al.*, 2006). A perturbation method known as the Method of Multiple Scales (MMS) was used for the stability analysis. The results showed that the coupling terms between the fuselage and rotor (i.e.: the periodic terms) lead to parametric instability of primary and second order.

The suppression of such instabilities can attained by adding dampers on the fuselage or on the blades. Over the last years, elastomeric lag dampers have been preferred to be incorporated to articulated rotors (Panda *et al.*, 1996). In the quest for reducing parts count, weight and maintenance costs, elastomeric lag dampers offer several advantages over conventional hydraulic dampers. Several authors have directed their research to the characterization of viscoelastic materials (i.e.: including nonlinear effects) (Gandhi and Chopra, 1996) and on the design of elastomeric dampers (Kunz, 1999; Brackbill, 2000; Kunz, 2002).

The design of elastomeric dampers is complex and it needs to be accurate in predicting the energy dissipated, since its principal function is to provide sufficient damping to prevent instability.

The viscoelastic materials are characterized by their dependency of the stiffness and damping with respect to the operational conditions (i.e.: frequency and amplitude of oscillations) and environmental condition (i.e.: temperature).

Several models have been developed for viscoelastic materials, both in frequency-domain and time-domain. Those, in frequency-domain, express the damping and stiffness by loss and storage moduli (i.e.: imaginary and real parts of the complex modulus).

Inserted in the group of modern models for viscoelastic materials, the fractional Zener model considers a general order of differentiation to the derivative operator (Lakes, 2009; Sales, 2012; Näsholm and Holm, 2013). This model leads to simple constitutive equations and has been used in different applications (Lakes, 2009; Näsholm and Holm, 2013).

The present work aims at treating the ground resonance phenomenon in helicopters with viscoelastic dampers on the fuselage and on the blades. For this Method of Multiple Scales is used. Further, a parametric study on the boundaries of ground resonance instability by assuming different levels of viscoelastic damping is developed. Conclusions and perspectives are finally presented.

2. MECHANICAL MODEL OF THE FUSELAGE-ROTOR SYSTEM

Figure 1 shows the mechanical model adopted for analyzing the ground resonance phenomenon in helicopters with hinged blades and under the aging effects. It is based on that used by (Sanches *et al.*, 2011; Sanches, 2011; Sanches *et al.*, 2012). The fuselage, modeled as a rigid body, contains one translational movement $x(t)$ along its longitudinal direction.
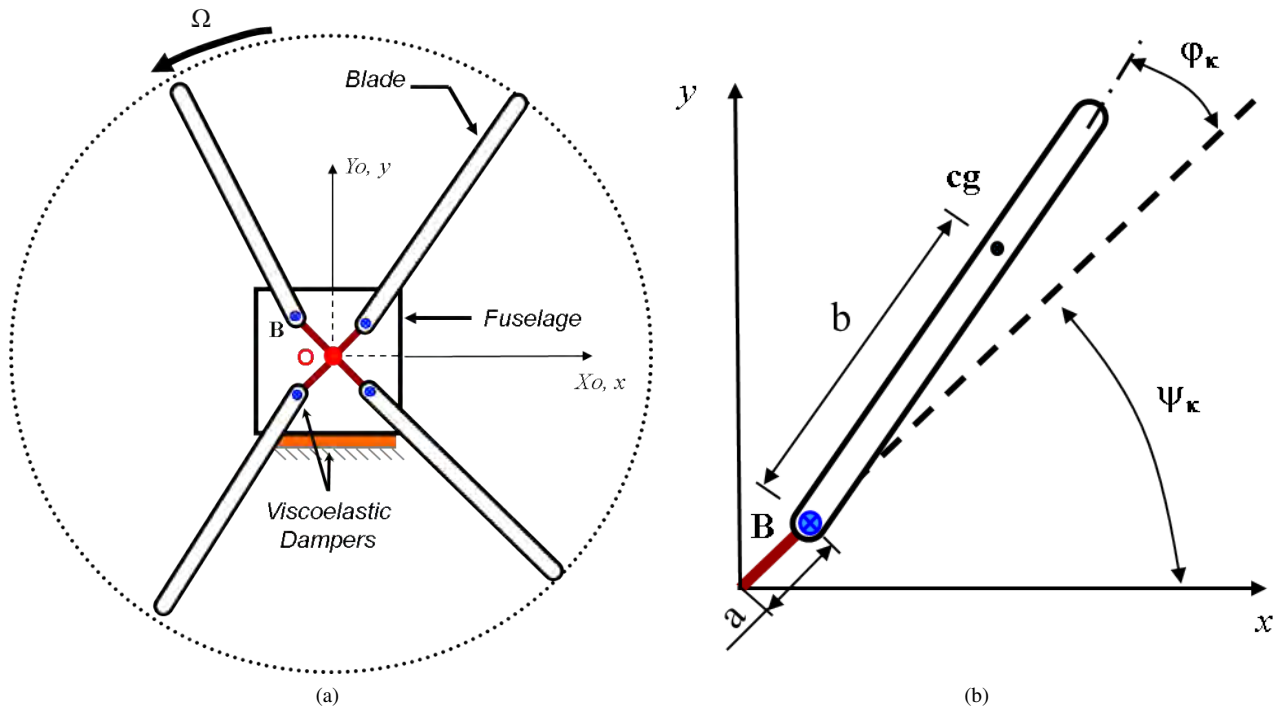

Figure 1: Sketch of the Mechanical System: (a) General View and (b) Blade View

The helicopter at its equilibrium position has the center of mass of the fuselage (point *O*) coincident with the origin of inertial reference frame (X_0, Y_0, Z_0).

The rotor head system is composed of one rigid rotor hub and an assembly of N_b blades. The blades have mass m_b and a moment of inertia I_{zb} around the z - axis located at its center of mass. The radius of gyration is denoted b. The kth blade owns an in-plane lead-lag motion defined by $\varphi_k(t)$ and an azimuth angle defined as $\zeta_k = 2\pi (k-1) / N_b$ with respect to the x - axis.

A rotational reference frame (x, y, z) is parallel to the inertial one and its origin is located at the geometric center of the rotor hub (coincident at point *O*). The rotating reference frame revolves at the same speed as the rotor, indicated by Ω.

The fuselage and the rotor head are connected to each other by a rigid shaft. Aerodynamic forces on the blades are not taken into account. Such an assumption is quite realistic since the helicopter is on the ground. In the present work, the rotor is composed of $N_b = 4$ blades.
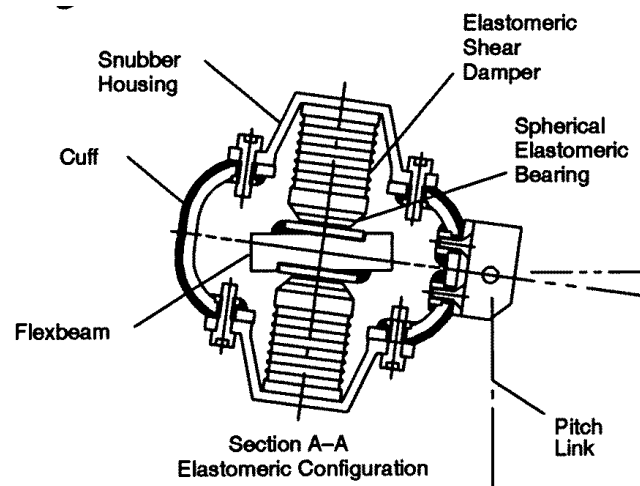
3. MODEL OF ELASTOMERIC DAMPERS

Figure 2 shows a scheme of an elastomeric lag damper. The principal elements of the elastomeric rotor configuration considered in this study is the flexbeam, spherical elastomeric bearing and the elastomeric shear damper.

The flexbeam and the spherical elastomeric bearing elements are directly connected to the blade and they give additional lag stiffness to blades. The elastomeric shear damper is composed of n bounded layers of viscoelastic materials. These layers are slightly deformed by the blade loads, under dynamic conditions.

Viscoelastic materials are characterized by the temporal dependency of the stress $\sigma(t)$ and strain $\epsilon(t)$. Experimental tests have shown that the response of viscoelastic materials to step strain is stress relaxation and the response to step stress is creep. Among different classical and modern models for these materials, the one used here is the Zener Fractional Model.

According to Lakes (2009), the time-domain and frequency-domain representation of Zener Fractional Model is represented in Eq.(1).

$$\sigma(t) + \tau^\alpha \frac{\mathrm{d}^\alpha \sigma(t)}{\mathrm{d}t^\alpha} = E_0 \epsilon(t) + \tau^\alpha E_\infty \frac{\mathrm{d}^\alpha \epsilon(t)}{\mathrm{d}t^\alpha} \tag{1a}$$

Figure 2: Schema of an Elastomeric Rotor Configuration (obtained from Panda *et al.* (1996))

$$E^* (\omega) = \frac{E_0 + E_\infty \left(I\omega\tau\right)^\alpha}{1 + \left(I\omega\tau\right)^\alpha}; \qquad G^* (\omega) = \frac{E^* (\omega)}{2 \left(1 + \nu\right)} \tag{1b}$$

where, E^* and G^* is the frequency-domain Young and shear complex modulus. E_0, E_∞, τ and α are parameters determined from curve-fitting of experimental data. They are dependent of the temperature. At 25^oC, the viscoelastic material ISD112$^{\text{TM}}$ from 3M has $E_0 = 1.2883$ [MPa], $E_\infty = 411.6754$ [MPa], $\tau = 0.7993\text{e} - 3$ [ms] and $\alpha = 0.64855$ (Sales, 2012).

The present work considers elastomeric dampers connected to blades and fuselage (see Fig. 1). Figure 3 illustrates, schematically, the geometry and the deformation of the viscoelastic materials of both dampers. The dashed lines represent the deformed configuration of the viscoelastic materials under the loads T (i.e.: twist moment) and F (i.e.: shear force).

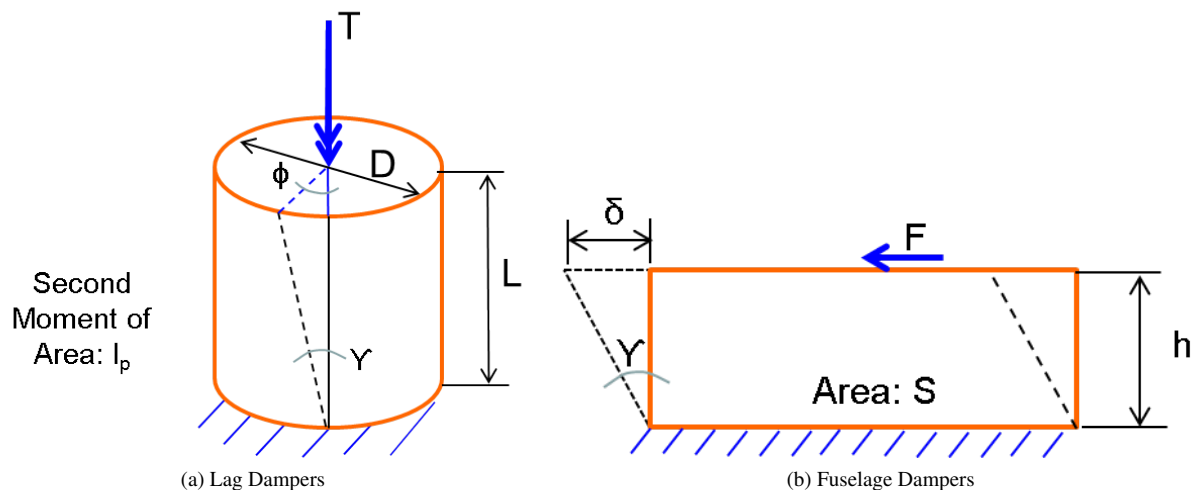(a) Lag Dampers

(b) Fuselage Dampers

Figure 3: Geometrical Characteristics and Deformations (dashed lines) of the Viscoelastic Material at: (a) Lag Dampers and (b) Fuselage Dampers

In Fig. 3a, the applied torque T rotates the blade with an angle φ. Since the blade root is attached at the upper surface of the viscoelastic material, this latter is twisted along its longitudinal axis. γ_{max} is the obtained shear strain.

Concerning Fig. 3b, the transmitted force F from the fuselage deforms the viscoelastic material with δ. The shear stain deformation of the material is $\gamma = \frac{\delta}{h}$.

The complex stiffness of the blade and fuselage elastomeric dampers are represented by Kv_b and Kv_{fX}, respectively. As mentioned above, due to viscoelastic material properties both Kv_b and Kv_{fX} are time dependent functions. In the frequency domain, the blade and fuselage complex stiffness might be obtained from the relations of the structural mechanics and expressed as:

- Blade Lag Damper:

$$Kv_b^* (\omega) = \frac{I_p}{L} G^* (\omega) = A G^* (\omega) \tag{2a}$$

- Fuselage Damper:

$$K v_{f\,X}^{*}(\omega) = \frac{S}{h}\, G^{*}(\omega) = B\, G^{*}(\omega) \tag{2b}$$

where, G^{*} is the complex modulus given in Eq.(1b). The parameters I_p, L, S and h are geometric properties of the elastomeric dampers (see Fig. 3). These geometrical parameters are included in the variables A and B.

4. GOVERNING EQUATIONS

In order to obtain the governing equations of motion, Lagrange equations are applied after formulating the kinetic and potential energies and the virtual work of the external forces and moments applied to of the dynamical system.

In Sanches *et al.* (2012), it can be found that the matrix equations of motion can be expressed as:

$$\mathbf{M}\,\ddot{\mathbf{u}} + \mathbf{G}\,\dot{\mathbf{u}} + \mathbf{K}\,\mathbf{u} = \mathbf{F_{ext}} \tag{3}$$

where,

$$\mathbf{u}(t) = \left\{ x(t) \quad \varphi_1(t) \quad \varphi_2(t) \quad \varphi_3(t) \quad \varphi_4(t) \right\}^{T} \tag{4}$$

$\mathbf{M}$, $\mathbf{G}$ and $\mathbf{K}$ correspond to the mass, damping and stiffness matrix, respectively. $\mathbf{F_{ext}}$ is equal to zero once all blades possess the same inertial and geometrical properties. The matrices are non-symmetric and non-diagonal due to the presence of periodic terms, as shown by Eq.(5).

$$\mathbf{M}(t) = \begin{bmatrix} 1 & -r_m \sin(\psi_1) & -r_m \sin(\psi_2) & -r_m \sin(\psi_3) & -r_m \sin(\psi_4) \\ -r_b \sin(\psi_1) & 1 & 0 & 0 & 0 \\ -r_b \sin(\psi_2) & 0 & 1 & 0 & 0 \\ -r_b \sin(\psi_3) & 0 & 0 & 1 & 0 \\ -r_b \sin(\psi_4) & 0 & 0 & 0 & 1 \end{bmatrix} \tag{5a}$$

$$\mathbf{G}(t) = \begin{bmatrix} 0 & -2\Omega r_m \cos(\psi_1) & -2\Omega r_m \cos(\psi_2) & -2\Omega r_m \cos(\psi_3) & -2\Omega r_m \cos(\psi_4) \\ 0 & 0 & 0 & 0 & 0 \\ 0 & 0 & 0 & 0 & 0 \\ 0 & 0 & 0 & 0 & 0 \\ 0 & 0 & 0 & 0 & 0 \end{bmatrix} \tag{5b}$$

$$\mathbf{K}(t) = \begin{bmatrix} \widetilde{\omega}_x^2 + \widehat{\omega}_x^2(t) & \Omega^2 r_m \sin(\psi_1) & \Omega^2 r_m \sin(\psi_2) & \Omega^2 r_m \sin(\psi_3) & \Omega^2 r_m \sin(\psi_4) \\ 0 & \widetilde{\omega}_b^2 + \widehat{\omega}_b^2(t) + \Omega^2 r_a^2 & 0 & 0 & 0 \\ 0 & 0 & \widetilde{\omega}_b^2 + \widehat{\omega}_b^2(t) + \Omega^2 r_a^2 & 0 & 0 \\ 0 & 0 & 0 & \widetilde{\omega}_b^2 + \widehat{\omega}_b^2(t) + \Omega^2 r_a^2 & 0 \\ 0 & 0 & 0 & 0 & \widetilde{\omega}_b^2 + \widehat{\omega}_b^2(t) + \Omega^2 r_a^2 \end{bmatrix} \tag{5c}$$

$$\mathbf{F}(t) = \left\{ 0 \quad 0 \quad 0 \quad 0 \quad 0 \right\}^{T} \tag{5d}$$

where,

$r_m = \frac{b\,m_b}{m_f + N_b\,m_b}$, $r_b = \frac{b\,m_b}{b^2\,m_b + I_{z_b}}$, $r_a^2 = a\,r_b$, $\psi_k = \Omega t + \zeta_k$, $\widehat{\omega}_x^2(t) = \frac{K v_{f\,X}(t)}{m_f + N_b\,m_b}$, $\widehat{\omega}_b^2(t) = \frac{K v_b(t)}{b^2\,m_b + I_{z_b}}$

Table 1 gives the approximated numerical data for a real helicopter.

Table 1: Numerical Data of the Helicopter

Fuselage		Rotor		
$m_f = 2902.9$ [Kg]	$m_{b\,k} = 31.9$ [Kg]	$a = 0.2$ [m]		$b = 2.5$ [m]
$\widetilde{\omega}_x = 6.0\,\pi$ [rad/s]	$\widetilde{\omega}_b = 3.0\,\pi$ [rad/s]	$I_{zb} = 259$ [Kg m^2]		

5. STABILITY ANALYSIS

The stability analysis of the periodic governing equation of motion - Eq.(3) - can be performed by using nonlinear techniques. Based on the development given by Sanches *et al.* (2012) for treating the ground resonance phenomenon with anisotropic rotor, the Method of Multiple Scale (MMS) is used.

The perturbation method MMS considers an asymptotic development on the time response functions of the dynamical system. Based on this, the variable $\mathbf{u}(t)$ has the form of:

$$u_n(t) = u_{n_0}(T_0, T_1) + \epsilon\, u_{n_1}(T_0, T_1) + \mathcal{O}(2),\, n = 1..5$$

where, ϵ is the bookkeeping parameter.

The periodic terms, except the fuselage and blade lag frequencies, are scaled to appear as parametric excitations at the first order of ϵ. For this purpose, the following substitutions $r_{m\,k} = \epsilon\alpha_k$ and $r_{b\,k} = \epsilon\beta_k$ are done.

Two sets of equations are obtained by grouping them as coefficients associated to increasing of ϵ (Sanches *et al.*, 2012). These sets of equations are described below.

5.1 Order ϵ^0 equations

The set of order ϵ^0 equations is represented by

$$\mathrm{D}_0^2\, u_{n_0} + \overline{\omega}_n^2\, u_{n_0} = 0,\, n = 1..5 \tag{6}$$

where D_0 indicates the partial derivative with respect to T_0. Note that the periodic terms do not appear in the equations since they were scaled up to the order ϵ^1. The natural frequency $\overline{\omega}_n^2$ is a time dependent function, as follows:

$$\overline{\omega}_1(t) = \sqrt{\widetilde{\omega}_x^2 + \widehat{\omega}_x^2(t)},\ \overline{\omega}_{k+1}(t) = \sqrt{\widetilde{\omega}_b + \widehat{\omega}_b^2(t) + r_a^2\Omega^2},\ k = 1..N_b$$

The linear set of order ϵ^0 equations represents the uncoupled fuselage/rotor system. Each generalised coordinate (fuselage translational movement and blade rotations) behaves as an independent oscillator.

The homogeneous response of the differential equation Eq.(6) is obtained in the frequency domain. From Eq.(2), Eq.(6) might be expressed as:

$$\left[s^2 + \widetilde{\omega}_x^2 + \frac{r_m}{b\,m_b} K v_{f\,X}^*(\omega)\right] U_{n_0}(\omega) = 0, n = 1 \tag{7}$$

$$\left[s^2 + \widetilde{\omega}_b^2 + \frac{r_b}{b\,m_b} K v_b^*(\omega) + r_a^2\Omega^2\right] U_{n_0}(\omega) = 0, n = 2..5 \tag{8}$$

where, $s = \mathrm{i}\,\omega$ and i indicates the imaginary unit.

The frequency domain equations of fuselage and blades, accordingly to Eqs.(7) and (8), are similar to that of a tuned mass damper with undamped natural frequency ω and damping factor ζ. Thus,

- Fuselage Equation

$$\widetilde{\omega}_x^2 + \frac{r_m}{b\,m_b} K v_{f\,X}^*(\omega) = \omega^2(1 + \mathrm{i}\,\zeta)^2 \tag{9a}$$

- Blade Equation

$$\widetilde{\omega}_b^2 + \frac{r_b}{b\,m_b} K v_b^* = \omega^2(1 + \mathrm{i}\,\zeta)^2 \tag{9b}$$

From Eq.(9a), the equivalent natural frequency ω_1 and damping factor ζ_1 of the fuselage are obtained. Similarly for the blades, from Eq.(9b), their natural frequencies $\omega_{2..5}$ and damping factors $\zeta_{2..5}$ are computed.

The homogeneous responses for the set of order ϵ^0 equations, Eq.(6), are trivial and take the form of

$$u_{n_0} = \frac{1}{2} C_n(T_1)\, \mathrm{e}^{(-\zeta_n\,\omega_n T_0)} \mathrm{e}^{(\mathrm{i}\,\omega_n T_0)} + [c.c.], \quad n = 1..5 \tag{10}$$

The term $C_n(T_1)$ is complex and [c.c.] represents the complex conjugate of the previous terms.

Sanches, L., Rade, D.A.
Influence of Viscoelastic Dampers on the Ground Resonance Instability of Helicopters

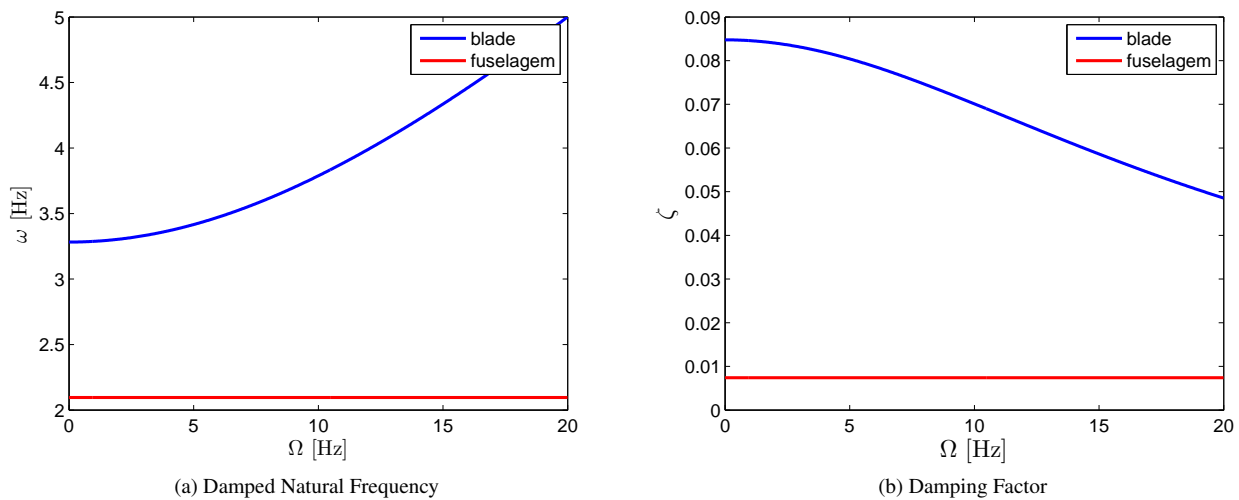(a) Damped Natural Frequency (b) Damping Factor

Figure 4: Evolution Dynamical Properties of the Fuselage and Blades with Viscoelastic Dampers: (a) Damped Natural Frequency and (b) Damping Factor

Figure 4 shows the evolution of the damped natural frequencies ω_n and damping ratios ζ_n of the fuselage and blade at the set of order ϵ^0 equations - see Eq.(6). The viscoelastic material properties used in the simulation are given in section 3 while the helicopter data are in Tab. 1. For instances, $A = 0.314$ and $B = 0.1$ (see Eq.(2)).

A common characteristic is observed for the damped natural frequency and damping factor of the fuselage in Fig. 4. ω_1 and ζ_1 are constant while Ω is varying. This is verified since the viscoelastic damper of the fuselage is not under the influence of the centrifugal force. However, such force strongly influences the viscoelastic dampers in the blades. One may note that the damped natural frequency of blades has increased while the damping factor decreases.

5.2 Order ϵ^1 equations

The set equations of order ϵ^1 are represented below.

$$D_0^2 u_{1_1} + \omega_1^2\, u_{1_1} = -2D_1 D_0 u_{1_0} +$$
$$\sum_{n=3}^{6} \left\{ \begin{array}{c} -\frac{1}{2}i^{(n-2)}\alpha_{n-2}D_0^2\, u_{n_0} e^{(i\Omega T_0)} + i^{(n-3)}\alpha_{n-2}\Omega D_0\, u_{n_0} e^{(i\Omega T_0)} \\ +\frac{1}{2}i^{(n-2)}\alpha_{n-2}\Omega^2\, u_{n_0} e^{(i\Omega T_0)} + [c.c.] \end{array} \right\} \tag{11a}$$

$$D_0^2 u_{n_1} + \omega_n^2 u_{n_1} = -2D_1 D_0 u_{n_0} - \frac{1}{2}i^{(n-2)}\beta_{n-2}D_0^2\, u_{1_0} e^{(i\Omega T_0)} \tag{11b}$$

$$- \frac{1}{2}i^{(n-3)}\beta_{n-2}D_0^2\, u_{2_0} e^{(i\Omega T_0)} + [c.c.], \ n = 3..6$$

The right-hand side of the above equations highlights the existence of external excitations that are totally dependent on the steady-state responses u_{n_0}.

It is not difficult to observe that depending on the rotor speed value, the external excitations of Eq.(11) might lead to a resonance condition. In this case, the resonance is called parametric resonance of first order.

Parametric resonances of first order in the dynamical system are detected when any combination of frequencies from the periodic excitation terms becomes equal to the natural frequency of the linear dynamical system.

Sanches *et al.* (2012) have employed the present technique to the analysis of the stability of helicopters on ground. Four parametric resonances of first order were found. Only two of them were unstable.

In the present work, based on the previous study mentioned above, the critical rotor speed Ω_{crit}, in which the parametric resonance can be unstable, is obtained when

$$\omega_1 = \Omega_{crit} - \omega_n \quad \Rightarrow \Omega_{crit} = \omega_1 + \omega_n, \quad n = 2..5 \tag{12}$$

The boundaries of ground resonance are determined by studying the stability of the parametric resonant case, through the solvability conditions (Sanches *et al.*, 2012). The solvability conditions, composed by the secular terms which must vanish, consist in a set of first order differential equations.
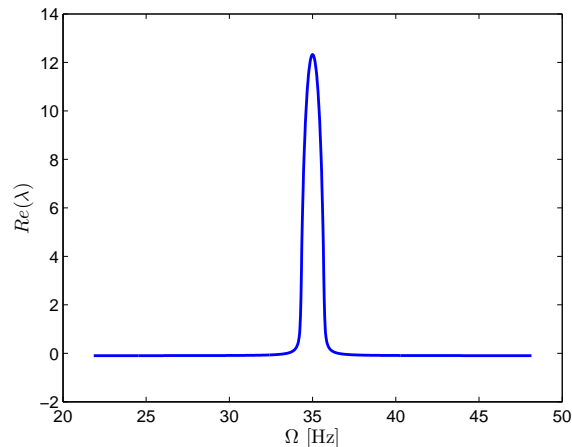
Figure 5: Stability of the Helicopter at Parametric Resonance of First Order - $\Omega = \omega_1 + \omega_n, \quad n = 2..5$

The stability of the dynamical system is obtained by observing the eigenvalues λ of the solvability conditions. For a stable system, the real part of λ must be negative.

A stability diagram of the helicopter at the parametric resonance of first order mentioned above is illustrated in Fig. 5, considering the same numerical data used in Fig. 4.

The ground resonance phenomenon occurs for Ω between 33.46 and 36.54 Hz. The maximum exponential growth factor obtained is 0.324.

6. PARAMETRIC ANALYSIS

The present work aims to verify the influence of the viscoelastic dampers on the boundaries of the helicopter instability. In this section, a parametric study on the ground resonance phenomenon is carried out by considering different levels of viscoelastic damping introduced in blades and fuselage.

For the accomplishment of such parametric study, different combinations of the geometrical parameters of the elastomeric dampers are assumed. That is, the constants A and B are considered in the ranges $[0.01, 0.1, 1, 5]$ and $[0.01, 0.1, 1, 5]$, respectively. For the simulation, the viscoelastic material properties are given in section 3 while the helicopter data are in Tab. 1.

Looking at the evolution of the fuselage damped natural frequency and the damping factor with respect to Ω, Fig. 6 illustrates that both are constants with respect to the rotor speed and they increase once B grows.

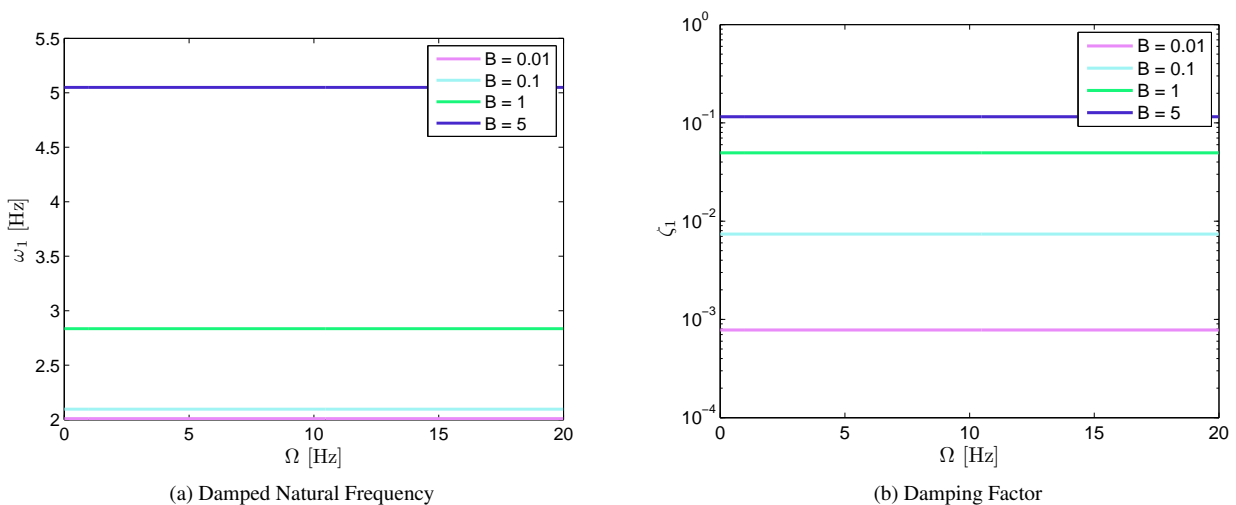(a) Damped Natural Frequency

(b) Damping Factor

Figure 6: Parametric Analysis on the Evolution of the Dynamical Properties of the Fuselage for Different Elastomeric Dampers: (a) Damped Natural Frequency and (b) Damping Factor

Concerning the blade natural frequency and damping factor, Fig. 7 shows a dependence of their values with respect to Ω. As it was evidenced in Fig. 4, by increasing the rotor speed, the blade natural frequency increases (due to the

centrifugal force) and the damping factor decreases.

However, analyzing the blade damping factor, this trend seems to occur only for low values of A. When higher level of the damping is considered, the damping factor takes its maximum value for the whole values of Ω.

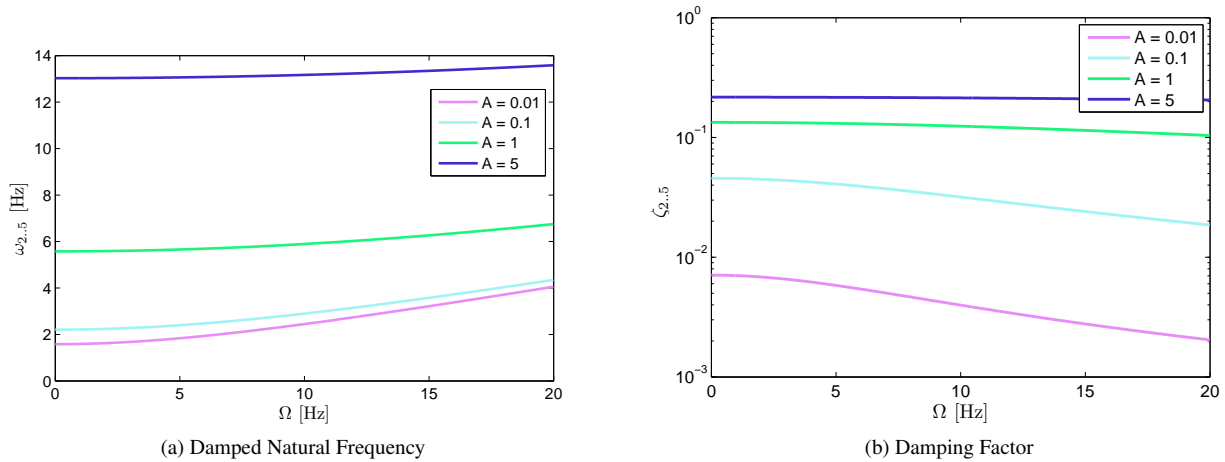(a) Damped Natural Frequency   (b) Damping Factor

Figure 7: Parametric Analysis on the Evolution of the Dynamical Properties of the Blades for Different Viscoelastic Dampers: (a) Damped Natural Frequency and (b) Damping Factor

The ground resonance stability is then analyzed for all combinations of viscoelastic damping in the fuselage and blades. The stability of the solvability conditions at the parametric resonance of first order, given by Eq.(12), is analyzed for each combination. The instability region is defined when $Re(\lambda) > 0$.

Figure 8 illustrates the boundaries of instability for different combinations of A and B. Table 2 summarizes the main results, namely the rotor speed (Ω_{max}) at which the exponential growth reaches its maximum value and the critical rotor speed width ($\Delta\Omega$) within which the instability occurs.
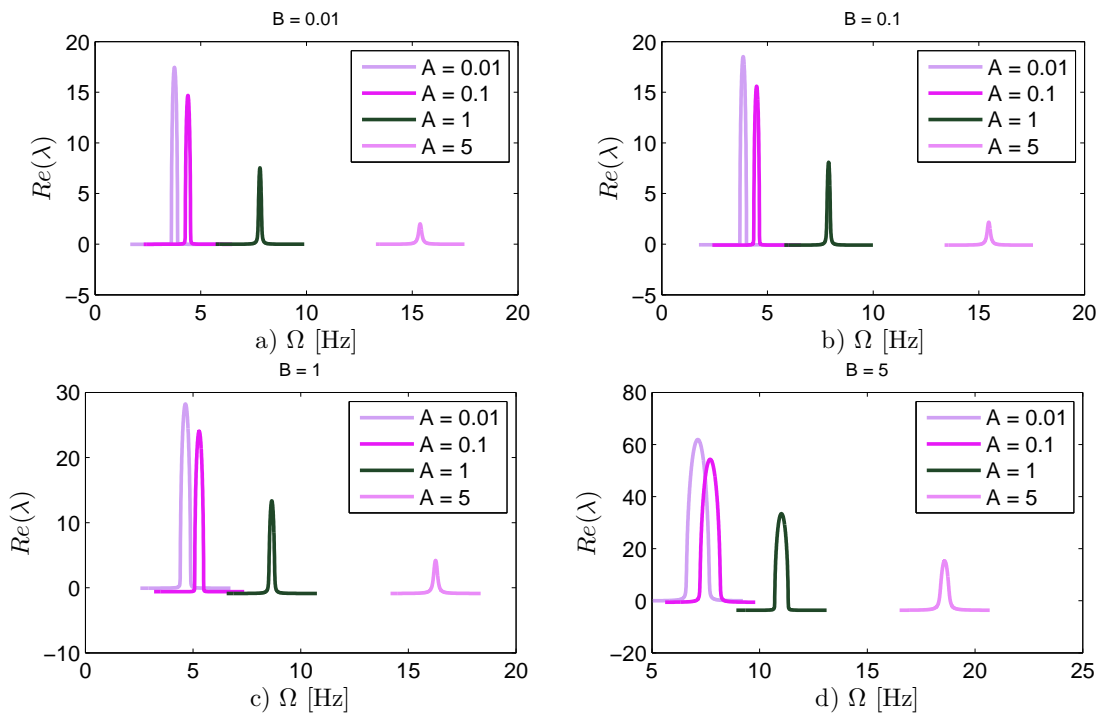

Figure 8: Parametric Stability Diagram for Different Combinations of Viscoelastic Dampers

Accordingly to Eq.(12), any increment in the natural frequencies of the blades or fuselage leads to increase of the Ω_{crit}. Thus, as verified previously in Figs. 6 and 7, the increment on the Ω_{crit} can be obtained depending on the selected level of the damping.

Table 2: Main Results from the Parametric Stability Analysis of Fig. 8

A		0.01	0.1	1	5
B = 0.01	$\Omega_{max}[Hz]$	3.75	4.39	7.8	15.43
	$\Delta\Omega$ [Hz]	0.4	0.72	1.42	1.54
B = 0.1	$\Omega_{max}[Hz]$	3.85	4.49	7.90	14.61
	$\Delta\Omega$ [Hz]	0.32	0.38	0.59	0.72
B = 1	$\Omega_{max}[Hz]$	4.65	5.29	8.66	16.27
	$\Delta\Omega$ [Hz]	0.89	0.46	0.35	0.38
B = 5	$\Omega_{max}[Hz]$	7.13	7.71	11.05	18.6
	$\Delta\Omega$ [Hz]	3.82	1.24	0.66	0.41

This fact is also reflected on the stability diagram. As shown in Tab.2, the Ω_{max} reaches high values when A or B increase.

Moreover, considering A constant and B varying, once high rotor speed is needed, higher kinetic energy is involved and higher exponential growth is reached, as observed from Fig. 8.

From Tab. 2, one observes that larger width of the instability regions are obtained when high discrepancy between A and B is reached. Nevertheless, the lowest exponential growth ($Re(\lambda)$) is obtained with the high discrepancies, when $A >> B$.

7. CONCLUSIONS

Over the last decades, elastomeric dampers have been preferred to be employed in rotor design for the prevention of the ground resonance instabilities in helicopters. The viscoelastic dampers have several advantages over conventional hydraulic ones.

The present work analyzes the helicopter dynamics considering viscoelastic dampers in the fuselage and in the blades. The periodic equations of motions of the helicopter, including the time dependent behavior of viscoelastic materials, have been treated with the Method of Multiple Scales.

A parametric study was developed on the stability of helicopters with different types (with respect to the dissipative power) of elastomeric dampers in the fuselage and blades.

The results have showed the dependency of instability region characteristics with respect to the set of elastomeric dampers selected. That is, the maximum exponential growth, the critical rotor speed and the width of the unstable zone (in terms of Ω) vary depending on the dissipative power of the dampers.

Further analysis will be devoted towards the influence of self-heating effect of viscoelastic dampers on the boundaries of the ground resonance instability.

8. ACKNOWLEDGEMENTS

9. REFERENCES

Brackbill, C.R., 2000. *Helicopter Rotor Aeroelastic Analysis Using a Refined Elastomeric Damper Model*. Ph.D. thesis, The Pennsylvania State University.

Donham, R., Cardinale, S. and Sachs, I., 1969. "Ground and Air Resonance Characteristics of a Soft In-Plane Rigid-Rotor System". *Journal of the American Helicopter Society*, Vol. 14, p. 33.

Driot, N., Lamarque, C. and Berlioz, A., 2006. "Theoretical and Experimental Analysis of a Base-Excited Rotor". *Journal of Computational and Nonlinear Dynamics*, Vol. 1.

Dufour, R. and Berlioz, A., 1998. "Parametric instability of a beam due to axial excitations and to boundary conditions". *Journal of Vibration and Acoustics*, Vol. 120, No. 2, pp. 461–467.

Gandhi, F. and Malovrh, B., 1999. "Influence of balanced rotor anisotropy on helicopter aeromechanical stability". *AIAA journal*, Vol. 37, No. 10, pp. 1152–1160.

Gandhi, F. and Chopra, I., 1996. "A time-domain non-linear viscoelastic damper model". *Smart Materials and Structures*, Vol. 5, No. 5, p. 517.

Hodges, D., 1979. "An aeromechanical stability analysis for bearingless rotor helicopters". *Journal of the American Helicopter Society*, Vol. 24, p. 2.

Kunz, D.L., 2002. "Nonlinear analysis of helicopter ground resonance". *Nonlinear Analysis: Real World Applica-*

Sanches, L., Rade, D.A.
Influence of Viscoelastic Dampers on the Ground Resonance Instability of Helicopters

tions, Vol. 3, No. 3, pp. 383 – 395. ISSN 1468-1218. doi:http://dx.doi.org/10.1016/S1468-1218(01)00037-2. URL `http://www.sciencedirect.com/science/article/pii/S1468121801000372`.

Kunz, D., 1999. "Elastomer modelling for usein predicting helicopter lag damper behavior". *Journal of Sound and Vibration*, Vol. 226, No. 3, pp. 585 – 594. ISSN 0022-460X. doi:http://dx.doi.org/10.1006/jsvi.1999.2222.

Lakes, R.S., 2009. *Viscoelastic Materials*. Cambridge University Press.

Lytwyn, R., Miao, W. and Woitsch, W., 1971. "Airborne and ground resonance of hingeless rotors". *Journal of the American Helicopter Society*, Vol. 16, p. 2.

Näsholm, S. and Holm, S., 2013. "On a fractional zener elastic wave equation". *Fractional Calculus and Applied Analysis*, Vol. 16, No. 1, pp. 26–50. ISSN 1311-0454. doi:10.2478/s13540-013-0003-1.

Panda, B., Mychalowycz, E. and Tarzanin, F.J., 1996. "Application of passive dampers to modern helicopters". *Smart Materials and Structures*, Vol. 5, No. 5, p. 509.

Sales, T.d.P., 2012. *Modelagem Numérico-computacional de Sistemas Multicorpos Flexíveis Contendo Materiais Viscoelásticos*. Master's thesis, Universidade Federal de Uberlândia.

Sanches, L., Michon, G., Berlioz, A. and Alazard, D., 2011. "Instability Zones for Isotropic and Anisotropic Multibladed Rotor Configurations". *Journal of Machine and Mechanism Theory*, Vol. "in press".

Sanches, L., Michon, G., Berlioz, A. and Alazard, D., 2012. "Parametrically excited helicopter ground resonance dynamics with high blade asymmetries". *Journal of Sound and Vibration*, Vol. In Press, No. 0, pp. –. ISSN 0022-460X. doi:10.1016/j.jsv.2012.03.029.

Sanches, L., 2011. *Helicopter Ground Resonance: Dynamical Modeling, Parametric Robustness Analysis and Experimental Validation*. Ph.D. thesis, ISAE - Institut Supérieur de l'Aéronautique et de l'Espace.

Wang, J. and Chopra, I., 1992. "Dynamics of helicopters in ground resonance with and without blade dissimilarities". In *AIAA Dynamics Specialists Conference, Dallas, TX*. pp. 273–291. ISSN 0146-3705.

10. RESPONSIBILITY NOTICE

The authors are the only responsible for the printed material included in this paper.